FEBS Letters 581 (2007) 1742–1750

Extracellular lipid droplets promote hemozoin crystallization in the gut of the blood fluke *Schistosoma mansoni*

Juliana B.R. Corrêa Soares[a], Clarissa M. Maya-Monteiro[b], Paula R.B. Bittencourt-Cunha[a], Geórgia C. Atella[a], Flávio A. Lara[c], Joana C.P. d'Avila[a], Diego Menezes[d], Marcos A. Vannier-Santos[d], Pedro L. Oliveira[a], Timothy J. Egan[e], Marcus F. Oliveira[a,*]

[a] *Instituto de Bioquímica Médica, Programa de Biologia Molecular e Biotecnologia, Universidade Federal do Rio de Janeiro, Cidade Universitária, Rio de Janeiro, RJ, Brazil*
[b] *Departamento de Fisiologia e Farmacodinâmica, Instituto Oswaldo Cruz, FIOCRUZ, Rio de Janeiro, Brazil*
[c] *Departamento de Micobacterioses, Instituto Oswaldo Cruz, FIOCRUZ, Rio de Janeiro, Brazil*
[d] *Instituto Gonçalo Moniz, FIOCRUZ, Salvador, Bahia, Brazil*
[e] *Department of Chemistry, University of Cape Town, Private Bag, Rondebosch, South Africa*

Received 5 December 2006; revised 8 February 2007; accepted 20 March 2007

Available online 30 March 2007

Edited by Hans Eklund

Abstract Hemozoin (Hz) is a heme crystal produced upon hemoglobin digestion as the main mechanism of heme disposal in several hematophagous organisms. Here, we show that, in the helminth *Schistosoma mansoni*, Hz formation occurs in extracellular lipid droplets (LDs). Transmission electron microscopy of adult worms revealed the presence of numerous electron-lucent round structures similar to LDs in gut lumen, where multicrystalline Hz assemblies were found associated to their surfaces. Female regurgitates promoted Hz formation in vitro in reactions partially inhibited by boiling. Fractionation of regurgitates showed that Hz crystallization activity was essentially concentrated on lower density fractions, which have small amounts of pre-formed Hz crystals, suggesting that hydrophilic–hydrophobic interfaces, and not Hz itself, play a key catalytic role in Hz formation in *S. mansoni*. Thus, these data demonstrate that LDs present in the gut lumen of *S. mansoni* support Hz formation possibly by allowing association of heme to the lipid–water interface of these structures.

Keywords: Hemozoin; Heme; Lipid droplets; *Schistosoma mansoni*

1. Introduction

Human schistosomiasis is a major health problem with an estimated 200 million people infected in 74 countries [1]. The major etiological agent of schistosomiasis is the trematode *Schistosoma mansoni* and the adult parasite stages digest huge amounts of host blood to meet their nutritional requirements [2]. During this process, hemoglobin derived from host erythrocytes is digested by a number of proteases into amino acids, peptides and heme which are released inside the parasite gut [3]. Heme constitutes an essential molecule to most living organisms [4], but once in a free state it acts as a pro-oxidant compound [5], and also interferes with phospholipid membrane stability [6]. Thus, the way which *S. mansoni* deal with free heme is of central importance in its physiology. In general, to overcome its toxicity, blood feeding organisms evolved efficient detoxification mechanisms in order to deal with heme [7], including the enzyme heme oxygenase [8] and heme binding proteins that prevent free radical formation [9,10]. Heme can be detoxified by its aggregation as in the gut of the cattle tick *Boophilus microplus* [11] and also in the gut of the mosquito *Aedes aegypti*, a vector of Dengue virus [7]. Many blood-feeding species, from malaria parasites to triatomine insects, detoxify heme into a dark brown crystal named hemozoin (Hz) [12–18]. In *Plasmodium*, *Rhodnius prolixus* and *S. mansoni*, Hz formation seems to represent the main heme detoxification pathway. Recent findings from our group corroborate this hypothesis, as in vivo treatment of *Schistosoma*-infected mice with chloroquine inhibits Hz formation in *S. mansoni*, reduces parasite burden and liver egg deposition in the infected animals [19].

Despite the efforts, little is known about how the process of Hz crystallization occurs and some possible catalysts were proposed such as proteins and Hz itself [20]. Nevertheless, several lines of evidence have converged to the possibility that lipids would play a major catalytic role in Hz formation by increasing heme solubility in acidic environments [19–29]. In line with these proposals, the existence of lipid bodies associated to *Plasmodium* food vacuoles was demonstrated and it was mainly composed of neutral lipids which were revealed to be efficient catalysts of Hz formation in vitro [25]. In fact, Egan and co-workers have recently shown that rapid and efficient Hz crystallization can be achieved in vitro in a lipid–water interface indicating that Hz formation could be performed through self-assembly of monomeric heme into dimeric iron-propionate forms [27]. Supporting these observations, Pisciotta and colleagues showed that neutral lipids surrounding Hz crystals are able to promote Hz crystallization in vitro [28]. Likewise, the presence of structures resembling lipid droplets in the gut lumen of both *S. mansoni* and *S. haematobium* was reported and some of them were found associated to an electrondense material at the droplet's surface [30,31]. The existence of hematin in these particles was also postulated but direct demonstration of this molecule and the significance of this interaction remained elusive [32]. Moreover, our group

*Corresponding author. Fax: +55 21 22708647.
E-mail address: maroli@bioqmed.ufrj.br (M.F. Oliveira).

0014-5793/$32.00
doi:10.1016/j.febslet.2007.03.054

showed that total lipids obtained from adult females of *S. mansoni* were efficient catalysts of Hz crystallization in vitro [19]. Multicrystalline assemblies of Hz were found at the surface of structures resembling lipid droplets in *S. mansoni* gut and also in close association to phospholipid membranes in *R. prolixus* midgut, suggesting that hydrophilic–hydrophobic interfaces would be essential to promote Hz crystallization [29]. Here, we studied the lipid droplets in the gut of the blood fluke *S. mansoni* and investigated their role in the Hz crystallization process.

2. Materials and methods

2.1. Chemicals and reagents

Hemin chloride, quinine, amodiaquine and Folin-phenol reagent were purchased from Sigma Chemical Co. (St. Louis, MO, USA). All other reagents were of analytical grade.

2.2. Parasites and animals

S. mansoni LE strain was maintained in *Biomphalaria glabrata* snails and in Syrian hamsters. Adult worms were obtained by mesenteric perfusion of Syrian hamsters 42 days after infection, as previously described [33]. To obtain unisexual worms, snails were infected with a single miracidium producing unisexual cercariae, which were then utilized for cervical injection in mice. Mice were treated in accordance with the Brazilian bio-safety guidelines and were kept in special care facilities.

2.3. Regurgitate isolation and fractionation

Worms obtained from mesenteric perfusion of mice were placed in ultrapure water at room temperature for 60 min and gently shaken every 5 min. After that, the sedimented worms were discarded and the supernatant, hereafter referred as "regurgitate", was collected. For fractionation, regurgitates were applied on the top of a discontinuous sucrose gradient (20%, 40% and 60% sucrose concentrations) and centrifuged at 16.000×*g* for 1 h at 4 °C (Beckman, Optima LE-80K ultracentrifuge, with a SW40 rotor). The five fractions produced (Top, 1, 2, 3 and 4) were collected and kept at −70 °C.

2.4. Hemozoin extraction and quantification

Hz was extracted from *S. mansoni* regurgitates from adult females of *S. mansoni*, or their isolated fractions, and quantified based on methods previously described [16]. Protein contents from regurgitates were measured using bovine serum albumin as a standard [34].

2.5. Total heme quantification

Total heme quantification was performed by incubating aliquots of regurgitates from adult females of *S. mansoni*, or their isolated fractions, in 0.1 N NaOH and determining the amount of heme spectrophotometrically at 400 nm as previously described [16].

2.6. Lipids

Total lipids were extracted in chloroform–methanol (1:2) from freshly obtained whole regurgitates of adult *S. mansoni* females as previously described [35]. For lipid extraction from regurgitate fractions, aliquots corresponding to 14.4 μg of protein were dialysed overnight at 4 °C against PBS using MWCO membranes (12.000–14.000) prior to chloroform–methanol. Neutral lipids were analyzed by high performance thin layer chromatography (HPTLC) on Silica gel 60 plates (Merck, Darmstadt, Germany) by applying 2 mg of total lipids extracted from regurgitates. Plates were firstly developed in 12 mL hexane: 8 mL ethyl ether: 0.2 mL acetic acid until the solvent front reached the middle of the plate and then, by a second mixture of 16 mL hexane:4 mL chloroform:0.2 mL acetic acid. For separation of phospholipids bidimensional TLC was carried out by applying 4 mg of total lipids extracted from regurgitates on Silica gel 250 plates (J.T. Baker, Phillipsburg, USA). Plates were firstly developed in 130 mL chloroform:60 mL methanol:15 mL ammonia and then 100 mL chloroform:20 mL methanol:40 mL of acetone:30 mL acetic acid:10 mL water. Plates were stained by spraying with phosphoric acid 8% (v/v) and copper sulfate 10% (w/v) and then heating at 250 °C for 10 min.

2.7. Hz crystallization assay

Samples corresponding to 20 μg of protein from whole or fractionated regurgitate, or 20 μg of lipids extracted from regurgitates, were incubated for 24 h at 37 °C in 0.5 M sodium acetate, pH 4.8, in the presence of 100 μM hemin and the produced Hz was extracted and quantified as described in item 2.4 above [19]. For reactions induced by regurgitate fractions, Hz crystallization activity was determined by subtracting the Hz produced in each fraction by their respective sucrose controls.

2.8. Transmission electron microscopy (TEM)

S. mansoni worms were fixed overnight at room temperature in 2.5% glutaraldehyde and 4% formaldehyde in 0.1 M sodium cacodylate buffer, pH 7.4 and processed for transmission electron microscopy as described earlier [29].

2.9. Spectrophotometry

UV–vis absorption spectra of whole regurgitates or their fractions were analysed in a GBC/UV-920 spectrophotometer (GBC).

2.10. Data analysis

Kinetics of Hz crystallization reactions induced by whole regurgitates or lipids were analysed by using linear least-squares fitting methods with the program GraphPad ©Prism 4.0. The data were fitted according to Avrami equation [26]:

$$v = v_0 + [v_\infty(1 - e^{-zt^n})]$$

where v is the amount of Hz formed (in nanomols), v_0 the amount of Hz present at the beginning of the reaction, v_∞ the amount of Hz formed at completion of the reaction, z the rate constant and n is the Avrami constant. For a process in which growth occurs along an interface between the two interconverting phases, as is likely to be the case for Hz formation in this model reaction, n takes an integer ranging between 1 and 4. Comparisons between groups were done by the non-paired Student's *t*-test or one-way ANOVA analysis of variance and a posteriori Tukey's test for pairwise comparisons. Differences of $P < 0.05$ were considered to be significant. Student's *t*-test, ANOVA, Tukey's test and correlation analysis were performed by GraphPad ©Prism 4.0 software.

3. Results and discussion

3.1. Crystal formation occurs at the surface of extracelullar lipid droplets in S. mansoni gut

The overall architecture of *S. mansoni* gut was firstly investigated by Morris [30], which demonstrated the presence of extracellular "lipid-like droplets" both in the gut lumen and within the epithelial cell cytoplasm. Interestingly, that early work considered these structures as different degrees of breakdown of blood components as they were associated with "dense caps" at the droplet's surface. In fact, Halton demonstrated that hematin was present only in the gut lumen of both sexes of *S. mansoni* but absent from the gut epithelial cells [32]. Interestingly, previous data demonstrated that worms treated with the immunomodulator cyclosporin-A caused profound changes on their morphology, characterized by the abnormal accumulation of iron-rich crystalline structures closely associated to lipid droplets (LDs) [36]. Since the catalysts involved in Hz formation remain unknown, our first step was to investigate the role of *S. mansoni* gut in Hz crystallization. When analysed by transmission electron microscopy (TEM), the gut of an adult male of *S. mansoni* shows red cell remnants and huge amounts of electron-lucent round structures, resembling

lipid droplets (LD) (Fig. 1A). A pattern quite similar was also observed for adult females in which LD of approximately 416.1 ± 68.7 nm (n = 32) in diameter, with or without the multicrystalline assemblies, were found lining the gut epithelial cells and microvilli (Fig. 1B). Similarly to what Morris found [35], we also observed the "dense caps" present at the surface of some of the LD, but a closer look indicated that these structures resembled the multicrystalline assemblies recently described by our group (Fig. 1C and Ref. [29]). Fig. 1C also shows an interesting feature of the crystallization process in which the multicrystalline assemblies were always found associated to the surface of LD, suggesting that Hz formation would be initiated at the hydrophilic–hydrophobic interface provided by the LDs and then growing toward the particles core. This is fully in agreement with recent findings of Egan and colleagues which demonstrated that Hz formation occurs rapidly and efficiently at organic–water and lipid–water interfaces [27]. In fact, we could observe crystals associated to LDs at different stages of crystallization (Fig. 1D), indicating that small "early" crystals were found at or near the LD surface and if the process of crystallization is sustained, these small crystals become larger "late" crystals which growth towards their cores. Interestingly, the involvement of LDs in Hz crystallization seems to explain the multicrystalline assem-

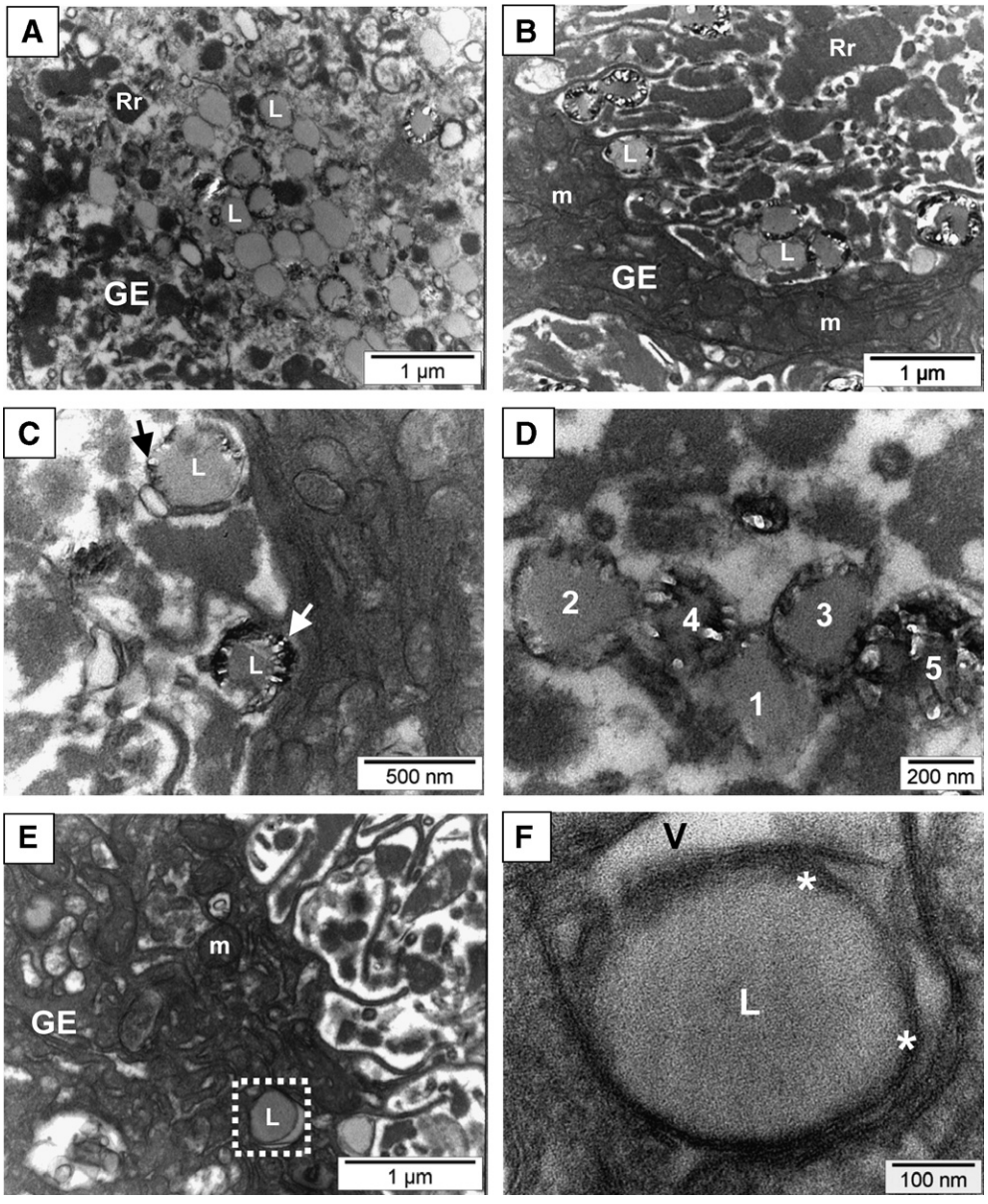

Fig. 1. Crystal formation occurs at lipid droplets (LDs) surface in the lumen of *S. mansoni* gut. Transmission electron microscopy of cross sections of adult males (A) and adult females (B–F) of *S. mansoni* gut. L – Lipid droplets; GE – Gut epithelium; Rr – Red blood cells remnants; m – mitochondria. Arrows in C indicate the association between crystals and lipid droplets (LDs). D – Panel shows several LDs associated with crystals in different stages of formation as indicated by numbers, the putative sequence of crystal growth (1 – very early to 5 – almost complete crystallized). E, F – LDs are present inside the gut epithelial cells. Panel E shows the presence of an intracellular LD in the gut epithelium. The dotted line in E represents the area magnified and depicted in F, showing an intracellular LD inside of a structure similar to a vacuole (V). This intracellular lipid particle seems to be wrapped by several layers of phospholipid membranes (asterisks). Bars denote the scale in nanometers.

blies previously observed by our group in *S. mansoni* gut [29]. Moreover, LDs associated with crystals were only found in gut lumen whereas epithelial gut cells only contain LDs devoid of crystals (Fig. 1E and F). An interesting observation is that intracellular LDs in epithelial gut cells were always found inside vacuolar structures and also wrapped by multilayers of double phospholipid membranes (Fig. 1F). The origin of the LDs remains unknown. These structures can be formed by lipids derived from blood cell breakdown or from gut epithelial cells. LDs observed inside these cells may be formed in the endocytic/autophagic pathway as were observed associated to multiple membranes presumably vacuolar (Fig. 1F).

3.2. Whole regurgitates of *S. mansoni* support Hz crystallization in vitro

Our group recently demonstrated that particulate fractions of whole homogenates of both adult males and females of *S. mansoni* were able to produce Hz in vitro in quinoline-sensitive reactions [19]. As very regularly shaped crystals were found associated with extracellular LD in *S. mansoni* gut, our next step was to obtain an enriched preparation of gut lumen, hereafter named regurgitate, to determine its capacity to induce Hz crystallization in vitro. Quantification of Hz, lipids and proteins in whole regurgitates of *S. mansoni* females show that this preparation is enriched with lipids and Hz as shown in Table 1. Regurgitates obtained from adult females are indeed derived from gut lumen as spectrophotometric analysis of these preparations exhibited an absorption spectrum very similar to Hz (Fig. 2A). Moreover, characterization of lipids present in *S. mansoni* LDs, by thin layer chromatography, revealed that this preparation contain essentially cholesterol (CHO), diacylglycerol (DAG) and triacylglycerol (TAG) as main neutral lipids (Fig. 2B) and phosphatidylcholine (PC) and phosphatidylethanolamine (PE) and phosphatidylserine (PS) as the main phospholipids (Fig. 2C). Also, regurgitates obtained from adult males and females promoted Hz crystallization, but females were much more efficient than males to catalyse this process (Fig. 2D). It is known that females of *S. mansoni* are dependent on pairing with males in order to complete sexual maturation [37], gene expression [38], red blood cell ingestion [39] and possibly Hz formation as unisexual infection with females produces stunted worms, which are sexually immature and have significantly less pigment than mated females [37]. Fig. 2D also shows that regurgitates obtained from females of unisexual infections were not able to promote Hz formation in vitro to the same extent as females of bisexual infections, suggesting that Hz crystallization activity present in whole regurgitates in females seems to be regulated by the presence of males. In fact, supporting these observations, Fig. 2E shows that females from unisexual infections produce much less Hz than male-paired ones, whereas males from unisexual infections showed a higher, but not statistically significant, Hz content than bisexual infections. Possibly, the reduced capacity to promote Hz crystallization by regurgitates from unisexual females could be related to reduced lipid content in this preparation. Thus, due to their high blood digestion capacity, Hz formation activity and also the efficiency by which whole regurgitates catalyze Hz crystallization in vitro, we investigated the Hz formation process only in females from bisexual infections in the subsequent experiments. As previously observed by our group, the activity responsible for Hz crystallization in vitro, in whole homogenates of adult females of *S. mansoni*, is completely heat and quinoline-sensitive [19]. Curiously, when whole regurgitates from adult females were previously boiled, we observed a significant inhibition of Hz crystallization activity, but much more resistant than that exhibited by whole homogenates (Fig. 3A and Ref. [19]), suggesting that Hz formation in *S. mansoni* seems not to require proteins on this process. Furthermore, in accordance to our previous data [19], incubation of whole regurgitates with quinine or amodiaquine abolished Hz formation in vitro. Lipids extracted from whole regurgitates also induced Hz crystallization in vitro in heat-resistant and quinoline-sensitive reactions, just like the activity previously described for lipids isolated from whole homogenates of adult females (Fig. 3B and Ref. [19]). Kinetic data for reactions induced by both regurgitates (Fig. 3C) and lipids (Fig. 3D) fit to the Avrami equation, showing a sigmoidal profile. This indicates that in the model system, Hz formation occurs via precipitation of heme, followed by slow conversion to the product in a process similar to that previously found in acetate and benzoate solutions [26,40]. The Avrami equation is used to model processes that occur via nucleation and growth. The value of the Avrami constant, n, can only take on integer values between 1 and 4. The value depends on whether nucleation is instantaneous (all nuclei are preformed at the beginning of the process), or sporadic (nuclei form throughout the process). It also depends on the geometry of growth from the nucleation sites. Table 2 shows the rate constants (z) and values of the Avrami constant for both regurgitate and lipid-driven reactions. When the data for regurgitates were averaged and then fitted to the Avrami equation, equally good fits were obtained with $n = 2$ and $n = 3$ (giving identical r^2 values). For lipid-driven reactions, data were clearly better modelled with $n = 2$. It therefore seems likely that $n = 2$ rather than 3 in the case of regurgitates. This can be interpreted in one of two ways. If instantaneous nucleation occurs, then crystal growth occurs via spreading areas in the precipitated heme. If nucleation is sporadic, then crystal growth occurs linearly from the nucleation sites. It seems somewhat more likely that nucleation would be sporadic and that the latter explanation would be correct. By selecting $n = 2$ for regurgitates, direct comparison between regurgitate and lipid-driven rate constants is possible. In the case of the former, the rate constant is considerably lower ($21 \pm 2\ h^{-2}$) than for the lipids ($74 \pm 18\ h^{-2}$). This difference may indicate that the surface area of lipid–water interfaces is larger in the case of lipids than in regurgitates. This interface appears to be the catalyst for Hz formation [27]. Alternatively, regurgitates may contain proteins that may bind heme, not allowing crystallization of Hz. Additionally, based on the recent demonstration by Pisciotta et al. [28] that lipids are associated with Hz crystals in the malaria parasite, there may not be sufficient lipid exposed to the

Table 1
Quantification of *S. mansoni* female regurgitate components

	Mean	S.E.	*n*
Hz (nmols heme/mL)	75.97	1.49	6
Lipids (mg/mL)*	12.94	6.02	7
Protein (mg/mL)	1.057	0.09	38

Hz, protein and total lipid contents of regurgitates obtained from adult females were determined as described in Section 2. Results were expressed as means ± S.E.M. and replicates.
*Student's t-test, $P < 0.0001$, relative to protein levels.

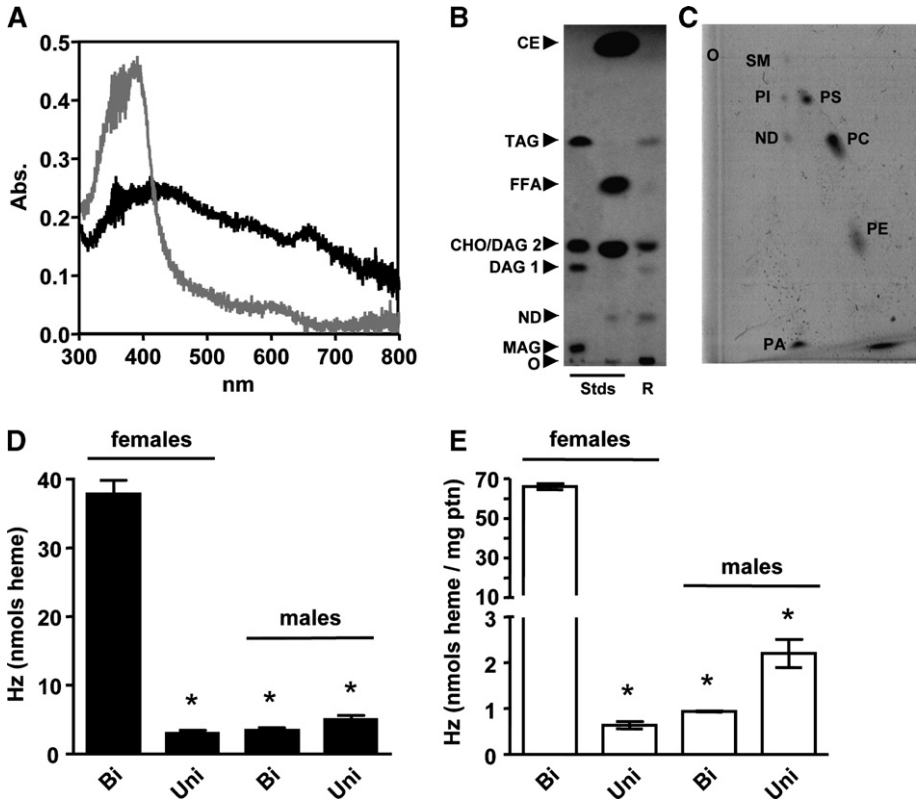

Fig. 2. Hz crystallization activity in whole regurgitate of adult females of *S. mansoni* is regulated by pairing. (A) UV–vis absorption analysis of regurgitate (130 μg ptn) obtained from *S. mansoni* females incubated in PBS (black line) or in the presence of 0.1 N NaOH (grey line). (B) High performance thin layer chromatography (TLC) of regurgitate (R) and standards of neutral lipids (Stds) applied at the origin (O): MAG – monoacylglycerol; CE – cholesterol ester; TAG – triacylglycerol; FFA – free fatty acids; CHO – cholesterol; DAG 1 and 2 – diacylglycerol; ND – non-determined neutral lipid. (C) TLC of regurgitate phospholipids: PC – phosphatidylcholine; PE – phosphatidylethanolamine; PS – phosphatidylserine; PI – phosphatidylinositol; PA – phosphatidic acid; SM – sphingomyelin; ND – non-determined phospholipid. (D) Evaluation of Hz crystallization activity in vitro using 20 μg of proteins from regurgitates of females or males obtained from bisexual (Bi) or unisexual (Uni) infections as catalysts in the presence of 100 μM heme in 0.5 M sodium acetate buffer, pH 4.8, 37 °C for 24 h as described in Section 2. (E) Evaluation of the Hz content in females or males from bisexual (Bi) or unisexual (Uni) infections. Hz was extracted, quantified and expressed as nmols of heme/mg of protein as described in Section 2. Results were expressed as means ± S.E.M. ($n = 4$). $^{*}P < 0.001$, for pairwise comparisons (one-way ANOVA and a posteriori Tukey's test) relative to bisexual females.

aqueous medium to support Hz formation. Finally, it should be noted that Avrami kinetics are an indication of solid heme precipitation, which may not occur in vivo where the heme could be continuously delivered to the lipid droplet interface. Thus differences could reflect the ease with which precipitated heme is delivered to the lipid environment in these in vitro systems.

3.3. Hydrophilic–hydrophobic interfaces play a central role in Hz crystallization in S. mansoni gut

In order to investigate heme association with regurgitate components and also its role on Hz formation, we performed a fractionation of whole regurgitates from adult females of *S. mansoni* by centrifugation in discontinuous sucrose gradient. This procedure resulted in five different density fractions, named top, 1, 2, 3 and 4 which exhibited remarkably distinct absorption spectra (Fig. 4A). Clearly, the lower density fractions showed high absorption regions near 400 nm (the Soret band) and also Q-bands absorption near 635 nm, whereas higher density fractions exhibited Soret absorption near 450 nm and also Q bands absorption near 660 nm (Fig. 4B, inset). Notice also that, fractions 3 and 4, especially, showed increased baseline absorption indicating that heme is found in an insoluble state. When fraction 4 was incubated with 0.1 M NaOH, a condition where Hz is converted to monomeric heme, we observed a spectrum identical to heme, suggesting that not only heme seems to be a major compound in this fraction but also that presence of degraded or unknown state of heme is unlikely (Fig. 4B). Thus, in general, the absorption spectra of lower density fractions were more similar to soluble free heme, whereas higher density fractions were more similar to Hz, indicating that some components of regurgitate interacts with heme, keeping it in a non-crystalline state which could then be converted to Hz. Conceivably, the lower density fractions would be composed of LDs associated with heme without crystals, or with nascent ones, whereas higher density fractions were those associated with heme essentially as Hz at LDs surface. We also evaluated the solubility of heme in these five different fractions of regurgitate by calculating the Soret/Q bands absorption ratio, which denotes whether heme is soluble (high ratios) or insoluble (lower ratios, near 1) as previously described [41]. In fact, lower density fractions of regurgitate exhibited higher Soret/Q bands absorption ratio of heme, from 3 to 7, suggesting the high spin iron in monomeric heme, whereas higher density fractions exhibited lower Soret/Q bands absorption ratio of heme, about 1, indicating that heme is out

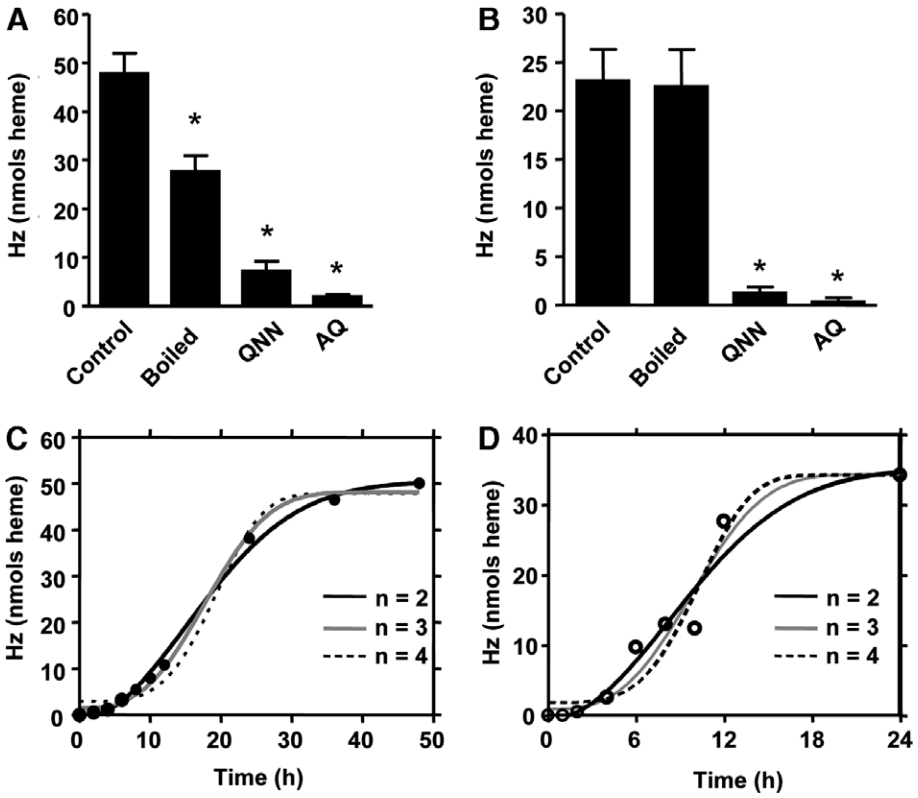

Fig. 3. Characterization of Hz crystallization activity induced by whole regurgitate or lipids. (A) Hz formation was induced by incubation of 20 μg of proteins from female regurgitates with 100 μM heme in 0.5 M sodium acetate buffer, pH 4.8, 37 °C for 24 h as described in Section 2. Control, previously to incubation with heme, regurgitate was heated for 30 min at 37 °C; boiled, previously to incubation with heme, regurgitate was boiled for 30 min at 100 °C; QNN, reactions with control regurgitate and heme were carried out in the presence of 50 μM of quinine; AQ, reactions with regurgitate and heme were carried out in the presence of 50 μM of amodiaquine. (B) Hz formation was induced by incubation of 20 μg of total lipids, extracted from female regurgitates, with 100 μM heme in 0.5 M sodium acetate buffer, pH 4.8, 37 °C for 24 h as described in Section 2. Control, previously to incubation with heme, lipids were heated for 30 min at 37 °C; boiled, previously to incubation with heme, lipids were boiled for 30 min at 100 °C; QNN, reactions with lipids and heme were carried out in the presence of 50 μM of quinine; AQ, reactions with lipids and heme were carried out in the presence of 50 μM of amodiaquine. (C) Avrami-fitted data of kinetics of Hz crystallization induced by whole regurgitate (20 μg of proteins) with 100 μM heme in 0.5 M sodium acetate buffer, pH 4.8, 37 °C for 48 h. The lines represent the fits ($n = 2$ – black line, $n = 3$ – grey line, or $n = 4$ – dashed line) of Avrami calculations. (D) Avrami-fitted data of kinetics of Hz crystallization induced by lipids (20 μg) extracted from female regurgitates, with 100 μM heme in 0.5 M sodium acetate buffer, pH 4.8, 37 °C for 24 h. The lines represent the fits ($n = 2$ – black line, $n = 3$ – grey line, or $n = 4$ – dashed line) of Avrami calculations. Results are means ± S.E.M. ($n = 4$). *$P < 0.001$, for pairwise comparisons (one-way ANOVA and a posteriori Tukey's test) relative to control.

Table 2
Rate constants of Hz formation and values of the Avrami constant

Samples	r^2			n (fixed)	Rate $z/10^{-4}$ h^{-n}
	$n = 2$	$n = 3$	$n = 4$		
Regurgitate	0.9961	0.9961	0.9867	2	21 ± 2
Lipids	0.9517	0.9506	0.9387	2	74 ± 18

Lipids were more efficient catalysts of Hz crystallization than regurgitate. Data show the rate constants and values of the Avrami constant for Hz crystallization reactions induced by regurgitate or lipids obtained from data fits shown in Fig. 3C and D. For calculation details, refer to Section 2.10 of Section 2.

of solution in these fractions (Fig. 4B, inset). In line with the data presented above, the higher density fractions were rich in both total heme and Hz, the latter representing about 50% of total heme particularly in fractions 2, 3 and 4 (Fig. 4C). Moreover, quantification of total lipids extracted from regurgitate fractions indicated that, although non-significant, the Top fraction seems to have more lipids than higher density fractions (Fig. 4D). Hz crystallization activity of these fractions revealed that lower density ones, which had lower Hz content, were more efficient catalysts than higher density ones, which contains more Hz (Fig. 4E). A negative correlation between Hz crystallization activity and pre-formed Hz content in fractions was established ($r^2 = 0.5841$, $P < 0.0001$), indicating that neither proteins, nor Hz itself, were responsible for Hz formation in the gut of *S. mansoni* (Fig. 4F). In fact, pre-formed Hz crystals somehow affected Hz crystallization induced by regurgitate probably due to their presence at LD surface, impairing heme to associate with LD hydrophilic–hydrophobic interface resulting in a reduced efficiency of Hz crystallization induced by Hz crystals compared to LD-driven reactions (Fig. 4F). This proposal is reinforced by our measurements of lipid content in regurgitate fractions which showed only a tendency of decrease in the amount of lipids in higher density fractions (Fig. 4D), suggesting that the major component influencing Hz crystallization are not lipids depletion itself but, instead, the abscence of a hydrophilic–hydrophobic interface at LD surface due to the presence of Hz crystals in higher density fractions (Figs. 1C and D and 4A and C). This would mean

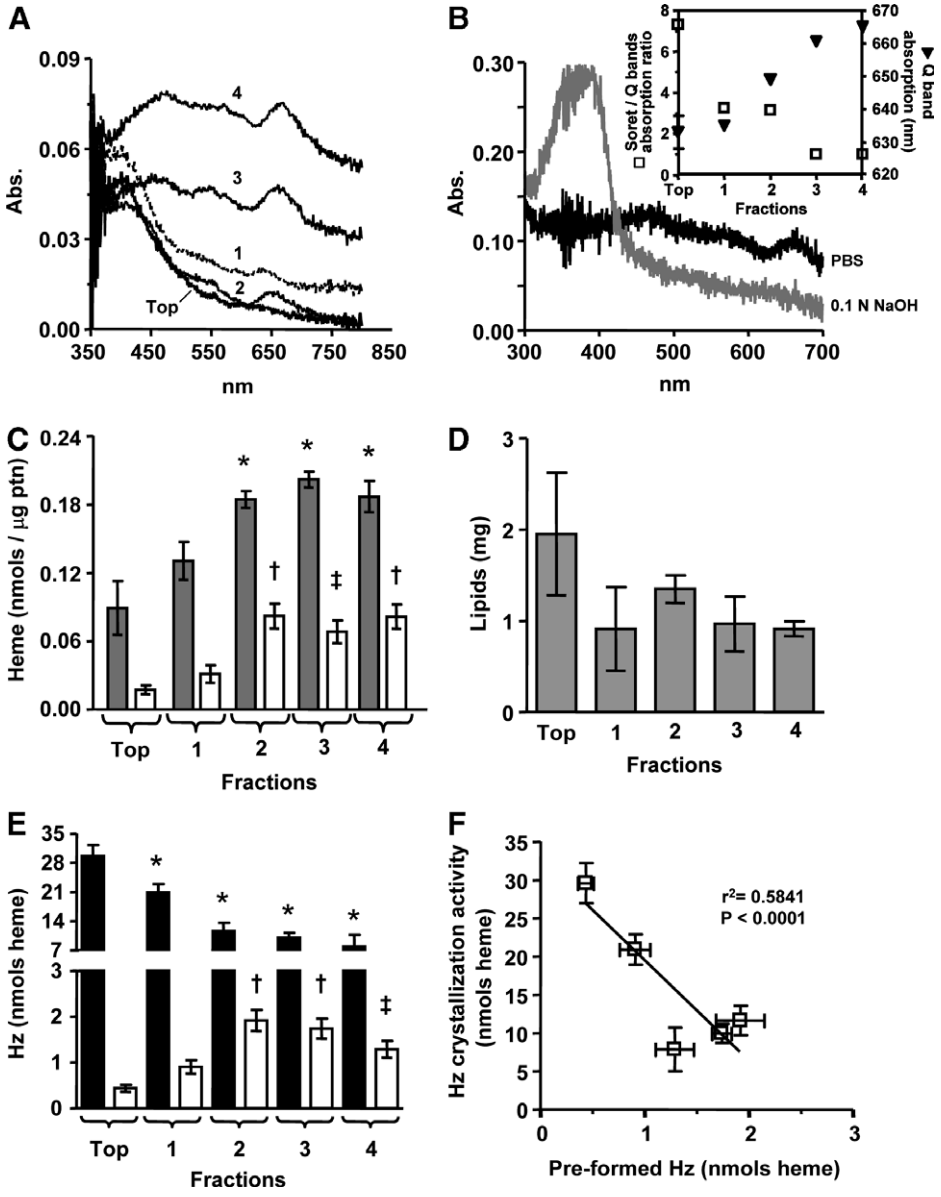

Fig. 4. Hz crystallization activity is associated with low density fractions of regurgitate. (A) UV–vis absorption spectra of 100 μL of regurgitate fractions (Top, 1, 2, 3 and 4), obtained from whole females regurgitate in sucrose gradient, incubated in the presence of 900 μL of 0.1 M $NaHCO_3$ pH 9.1. (B) UV–vis absorption spectra of fraction 4 (42 μg ptn) in PBS (black) or in 0.1 N NaOH (gray). Inset – The Soret/Q band absorption ratio (open squares) and Q-band red-shift (closed triangles) in regurgitate fractions. (C) Total heme (gray bars) and Hz (white bars) were quantified in the five regurgitate fractions and expressed as nmols heme/μg fraction protein. Hz and total heme were determined in each regurgitate fraction as described in Sections 2.4 and 2.5 of Section 2, respectively. $^{*}P < 0.001$ is relative to top gray bar, $^{\dagger}P < 0.001$ and $^{\ddagger}P < 0.01$ are relative to top white bar. (D) Total lipids extracted from regurgitate fractions (14.4 μg ptn) as described in Section 2. (E) Hz crystallization activity induced by 20 μg of proteins of each regurgitate fraction (black bars) and their respective pre-formed Hz content (white bars). $^{*}P < 0.001$ is relative to top black bar, $^{\dagger}P < 0.001$ and $^{\ddagger}P < 0.01$ are relative to top white bar. (F) Correlation ($r^2 = 0.5841$, $P < 0.0001$) between Hz crystallization activity of regurgitate fractions and their respective pre-formed Hz contents, using data from this figure E. In all figures, results were expressed as means ± S.E.M. ($n = 4$) and statistical differences were calculated by pairwise comparisons (one-way ANOVA and a posteriori Tukey's test).

that heme would be differently associating to LD, depending on the absence or presence of Hz crystals at LD surface, which would directly affect the rate by which heme is crystallized into Hz (Fig. 4E). Indeed, the kinetics of regurgitate and lipid-driven reactions, showed in Fig. 3C and D, indicate that despite having more lipids (20 μg protein added, corresponding to about 240 μg lipids) regurgitates were less efficient as a promoter of Hz crystallization than extracted lipids (20 μg lipids added), strenghten the idea that hydrophilic–hydrophobic interfaces present in LD seems to play a major catalytic role in Hz formation in *S. mansoni* gut.

The results shown here unambiguously demonstrate that Hz formation in the gut of *S. mansoni* occurs in LD and that lipids present in this structure play a key catalytic role in this process. Additionally, we provide further evidence to support the proposal that Hz crystallization occurs at lipid–water interfaces as not only Hz crystals were clearly seen at LD surfaces in *S. mansoni* gut (Fig. 1D) but also Hz crystallization is associated

to lipids availability at LD surface, as high density fractions, enriched with Hz crystals, were less effective in promoting Hz crystallization than low density fractions (Fig. 4E and F). Possibly, the lipid–water interfaces present at LD surfaces would facilitate the transition of hydrated monomeric free heme to dehydrated dimers of heme precursors of Hz by firstly solubilizing heme in acidic environments, thus avoiding precipitation into amorphous heme aggregates, followed by removal of the axial water bound to central iron, considered the limiting step of Hz formation [26,27]. In this context, environments which allow water removal from heme, i.e. phospholipid membranes, LD surfaces, hydrophobic pockets of lipoproteins, would be potential candidates to promote Hz crystallization. However, the picture is complex. For example, erythrocyte membranes do not promote Hz formation in contrast to perimicrovillar membranes of the *Rhodnius* midgut [42]. Studies under non-physiological conditions provide further evidence of the complexity of the process. For example, benzoic acid stimulates Hz formation without solubilizing heme under acidic condition [40]. Here, Hz formation appears to be stimulated through disruption of both hydrogen bonding and heme π-stacking by itself hydrogen bonding and forming π–π interactions with heme which may then allow rearrangement of the heme molecules to form Hz. On the other hand, preliminary results from our group indicate that solubilization of heme by organic solvents in acidic medium correlates with increased capacity to form Hz (data not shown). An important unknown feature is whether organisms have a specific mechanism for delivering heme to the lipid–water interface, as Hz formation at such an interface is vastly faster than that which occurs when heme is allowed to first precipitate in aqueous medium [27].

Our data suggest that the increment of heme solubility in the acidic environment of *S. mansoni* gut [43] would occur through its association with LDs surface, possibly due to its amphiphilic nature, allowing very rapid heme dehydration through the displacement of axial water molecule bound to the central heme iron followed by its dimerization [26,27]. Therefore, the presence of phospholipids and neutral lipids in LD would form a hydrophilic–hydrophobic interface facilitating Hz crystallization. In fact, the hydrophilic–hydrophobic interface-mediated catalysis seems to be more efficient than autocatalytic Hz-driven, or eventually protein-mediated Hz crystallization as high density regurgitate fractions, enriched of Hz crystals (Fig. 4C), proved to be weak promoters of Hz formation. Thus, this process seems to occur through the same mechanism in different organisms in which neutral lipids wrapping Hz crystals in *Plasmodium* food vacuoles, perimicrovillar membranes in triatomines [14,15,29] and LDs in *S. mansoni* (Fig. 1 and Ref. [29]) seems to be essential to promote heme solubilization and dimerization in the acidic environment where its is released in the digestive tract of these organisms. In fact, recent data from the literature demonstrated that under physiological conditions, Hz crystallization was induced rapidly and spontaneously in vitro near long chain alcohol/water and lipid/water interfaces [27]. Thus, regulation of the water content in the reaction medium seems to play a key role in Hz formation possibly, by facilitating the transition of hydrated heme to heme dimer precursors of Hz. Whatever the case, attempts to elucidate the contribution of hydrophilic–hydrophobic interfaces in Hz crystallization are currently being investigated in our lab.

In conclusion, we show that Hz crystallization in *S. mansoni* gut occur at the surface of extracellular LDs and that lipids present in this structure seem to play a key catalytic role, possibly by providing a hydrophilic–hydrophobic interface to allow heme dehydration, solubilization and then crystallization into Hz. These findings provide important information concerning formation of Hz crystals and open new perspectives for drug development against schistosomiasis placing the hydrophilic–hydrophobic interface of LDs as an important environment to target Hz formation.

Acknowledgements: We are grateful to Mr. Claudio P. Figueira, Mrs. Elisangela Sodré and Mrs. Maria Marta Freire for excellent technical assistance and to Dr. Franklin D. Rumjanek (IBqM, UFRJ) for the *S. mansoni* facility. This investigation received financial support from the UNICEF/UNDP/World Bank/WHO Special Programme for Research and Training in Tropical Diseases through the South–South Initiative Programme (A60265), CNPq, FAPERJ, FUJB, CAPES, FAPESB and the Third World Academy of Sciences (TWAS). M.F.O., P.L.O. and M.A.V.S. are research scholars from CNPq. P.L.O. is a Howard Hughes Medical Institute International research scholar.

References

[1] World Health Organization (2002) TDR Strategic Direction for Research: Schistosomiasis, World Health Organization, Geneve.
[2] Lawrence, J.D. (1973) The ingestion of red blood cells by *Schistosoma mansoni*. J. Parasitol. 59, 60–63.
[3] Kloetzel, K. and Lewert, R.M. (1966) Pigment formation in *Schistosoma mansoni* infections in the white mouse. Am. J. Trop. Med. Hyg. 15, 28–31.
[4] Ponka, P. (1999) Cell biology of haem. Am. J. Med. Sci. 318, 241–256.
[5] Davies, M.J. (1988) Detection of peroxyl and alkoxyl radicals produced by reaction of hydroperoxides with heme-proteins by electron spin resonance spectroscopy. Biochim. Biophys. Acta 964, 28–35.
[6] Schmitt, T.H., Frezzatti Jr., W.A. and Schreier, S. (1993) Hemin-induced lipid membrane disorder and increased permeability: a molecular model for the mechanism of cell lysis. Arch. Biochem. Biophys. 307, 96–103.
[7] Graca-Souza, A.V., Maya-Monteiro, C., Paiva-Silva, G.O., Braz, G.R., Paes, M.C., Sorgine, M.H., Oliveira, M.F. and Oliveira, P.L. (2006) Adaptations against heme toxicity in blood-feeding arthropods. Insect. Biochem. Mol. Biol. 36, 322–335.
[8] Paiva-Silva, G.O., Cruz-Oliveira, C., Nakayasu, E.S., Maya-Monteiro, C.M., Dunkov, B.C., Masuda, H., Almeida, I.C. and Oliveira, P.L. (2006) A heme-degradation pathway in a blood-sucking insect. Proc. Natl. Acad. Sci. USA 103, 8030–8035.
[9] Maya-Monteiro, C.M., Daffre, S., Logullo, C., Lara, F.A., Alves, E.W., Capurro, M.L., Zingali, R., Almeida, I.C. and Oliveira, P.L. (2000) HeLp, a heme lipoprotein from the hemolymph of the cattle tick, *Boophilus microplus*. J. Biol. Chem. 275, 36584–36589.
[10] Dansa-Petretski, M., Ribeiro, J.M., Atella, G.C., Masuda, H. and Oliveira, P.L. (1995) Antioxidant role of *Rhodnius prolixus* haem-binding protein. Protection against haem-induced lipid peroxidation. J. Biol. Chem. 270, 10893–10896.
[11] Lara, F.A., Lins, U., Paiva-Silva, G., Almeida, I.C., Braga, C.M., Miguens, F.C., Oliveira, P.L. and Dansa-Petretski, M. (2003) A new intracellular pathway of haem detoxification in the midgut of the cattle tick *Boophilus microplus*: aggregation inside a specialized organelle, the hemosome. J. Exp. Biol. 206, 1707–1715.
[12] Slater, A.F.G., Swiggard, W.J., Orton, B.R., Flitter, W.D., Goldberg, D.E., Cerami, A. and Henderson, G.B. (1991) An iron-carboxylate bond links the haem units of malaria pigment. Proc. Natl. Acad. Sci. USA 88, 325–329.
[13] Oliveira, M.F., Silva, J.R., Dansa-Petretski, M., de Souza, W., Lins, U., Braga, C.M.S., Masuda, H. and Oliveira, P.L. (1999) Haem detoxification by an insect. Nature 400, 517–518.
[14] Oliveira, M.F., Silva, J.R., Dansa-Petretski, M., de Souza, W., Braga, C.M.S., Masuda, H. and Oliveira, P.L. (2000) Hemozoin formation in the midgut of the blood sucking insect *Rhodnius prolixus*. FEBS Lett. 477, 95–98.

[15] Oliveira, M.F., Gandara A.C.P., Braga, C.M.S., Silva J.R., Mury, F.B., Dansa-Petretski, M., Menezes, D., Vannier-Santos M.A., Oliveira, P.L. (2007) Heme crystallization in the midgut of triatomine insects. Comp. Biochem. Physiol. C., in press.
[16] Oliveira, M.F., d'Avila, J.C.P., Torres, C.R., Oliveira, P.L., Tempone, A.J., Rumjanek, F.D., Braga, C.M.S., Silva, J.R., Petretski, M.D., Oliveira, M.A., Souza, W. and Ferreira, S.T. (2000) Hemozoin in *Schistosoma mansoni*. Mol. Biochem. Parasitol. 111, 217–221.
[17] Chen, M.M., Shi, L. and Sullivan Jr., D.J. (2001) *Haemoproteus* and *Schistosoma* synthesize haem polymers similar to *Plasmodium* hemozoin and β-hematin. Mol. Biochem. Parasitol. 113, 1–8.
[18] Pisciotta, J.M., Ponder, E.L., Fried, B. and Sullivan, D. (2005) Hemozoin formation in *Echinostoma trivolvis* rediae. Int. J. Parasitol. 35, 1037–1042.
[19] Oliveira, M.F., d'Avila, J.C.P., Tempone, A.J., Soares, J.B.R., Rumjanek, F.D., Ferreira-Pereira, A., Ferreira, S.T. and Oliveira, P.L. (2004) Inhibition of heme aggregation by chloroquine reduces *Schistosoma mansoni* infection. J. Infect. Dis. 190, 843–852.
[20] Egan, T.J. (2002) Physico-chemical aspects of hemozoin (malaria pigment) structure and formation. J. Inorg. Biochem. 91, 19–26.
[21] Bendrat, K., Berger, B.J. and Cerami, A. (1995) Haem polymerization in malaria. Nature 378, 138.
[22] Dorn, A., Vippagunta, S.R., Matile, H., Bubendorf, A., Vennerstrom, J.L. and Ridley, R.G. (1998) A comparison and analysis of several ways to promote haematin (haem) polymerisation and an assessment of its initiation in vitro. Biochem. Pharmacol. 55, 737–747.
[23] Fitch, C.D., Cai, G.Z., Chen, Y.F. and Shoemaker, J.D. (1999) Involvement of lipids in ferriprotoporphyrin IX polymerization in malaria. Biochim. Biophys. Acta 1454, 31–37.
[24] Hempelmann, E., Motta, C., Hughes, R., Ward, S.A. and Bray, P.G. (2003) *Plasmodium falciparum*: sacrificing membrane to grow crystals? Trends Parasitol. 19, 23–26.
[25] Jackson, K.E., Klonis, N., Ferguson, D.J., Adisa, A., Dogovski, C. and Tilley, L. (2004) Food vacuole-associated lipid bodies and heterogeneous lipid environments in the malaria parasite, *Plasmodium falciparum*. Mol. Microbiol. 54, 109–122.
[26] Egan, T.J., Mavuso, W.M. and Ncokazi, K.K. (2001) The mechanism of β-hematin formation in acetate solution. Parallels between hemozoin formation and biomineralization processes. Biochemistry 40, 204–213.
[27] Egan, T.J., Chen, J.Y., de Villiers, K.A., Mabotha, T.E., Naidoo, K.J., Ncokazi, K.K., Langford, S.J., McNaughton, D., Pandiancherri, S. and Wood, B.R. (2006) Haemozoin (β-haematin) biomineralization occurs by self-assembly near the lipid/water interface. FEBS Lett. 580, 5105–5110.
[28] Pisciotta, J.M., Coppens, I., Tripathi, A.K., Scholl, P.F., Shuman, J., Bajad, S., Shulaev, V. and Sullivan, D.J. (2007) The role of neutral lipid nanospheres in *Plasmodium falciparum* haem crystallization. Biochem. J. 402, 197–204.
[29] Oliveira, M.F., Kycia, S.W., Gómez, A., Kosar, A.J., Bohle, D.S., Hempelmann, E., Menezes, D., Vannier-Santos, M.A., Oliveira, P.L. and Ferreira, S.T. (2005) Structural and morphological characterization of hemozoin produced by *Schistosoma mansoni* and *Rhodnius prolixus*. FEBS Lett. 579, 6010–6016.
[30] Morris, G.P. (1968) Fine structure of the gut epithelium of *Schistosoma mansoni*. Experientia 24, 480–482.
[31] Sodeman, T.M., Sodeman Jr., W.A. and Schnitzer, B. (1972) Lamellar structures in the gut of *Schistosoma* haematobium. Ann. Trop. Med. Parasitol. 66, 475–478.
[32] Halton, D.W. (1967) Observations on the nutrition of digenetic trematodes. Parasitology 57, 639–660.
[33] Smithers, S.R. and Terry, R.J. (1965) The infection of laboratory hosts with cercariae of *Schistosoma mansoni* and the recovery of adult worms. Parasitology 55, 695–700.
[34] Lowry, O.H., Rosebrough, N.J., Farr, A.L. and Randall, R.J. (1951) Protein measurement with the Folin phenol reagent. J. Biol. Chem. 193, 265–275.
[35] Bligh, E.G. and Dyer, W.J. (1959) A rapid method of total lipid extraction and purification. Can. J. Biochem. Physiol. 37, 911–917.
[36] Munro, G.H. and McLaren, D.J. (1990) *Schistosoma mansoni*: morphology and ultrastructure of adult worms recovered from cyclosporin A-treated mice. Parasitology 100, 19–28.
[37] Popiel, I. (1986) The reproductive biology of schistosomes. Parasitol. Today 2, 10–19.
[38] Grevelding, C.G., Sommer, G. and Kunz, W. (1997) Female-specific gene expression in *Schistosoma mansoni* is regulated by pairing. Parasitology 115, 635–640.
[39] Gupta, B.C. and Basch, P.F. (1987) The role of *Schistosoma mansoni* males in feeding and development of female worms. J. Parasitol. 73, 481–486.
[40] Egan, T.J. and Tshivhase, M.G. (2006) Kinetics of β-haematin formation from suspensions of haematin in aqueous benzoic acid. Dalton Trans. 42, 5024–5032.
[41] Huy, N.T., Kamei, K., Yamamoto, T., Kondo, Y., Kanaori, K., Takano, R., Tajima, K. and Hara, S. (2002) Clotrimazole binds to heme and enhances heme-dependent hemolysis: proposed antimalarial mechanism of clotrimazole. J. Biol. Chem. 277, 4152–4158.
[42] Silva, J.R., Mury, F.B., Oliveira, M.F., Oliveira, P.L., Silva, C.P., Dansa-Petretski, M. (2007). Perimicrovillar membranes promote hemozoin formation into *Rhodnius prolixus* midgut. Insect. Biochem. Mol. Biol., in press.
[43] Bogitsh, B.J. and Davenport, G.R. (1991) The in vitro effects of various lysosomotropic agents on the gut of *Schistosoma mansoni* schistosomula. J. Parasitol. 77, 187–193.